Applications of two-photon absorption in silicon

XINZHU SANG[a,b*] EN-KUANG TIEN[b], OZDAL BOYRAZ[b]

[a]Key Laboratory of Optical Communication and Lightwave Technologies (MOE), Institute of Optical Communication and Optoelectronics, Beijing University of Posts and Telecommunications, Beijing, 100876, China
[b]Department of Electrical Engineering & Computer Science, University of California, Irvine, CA, 92697, USA

The main theoretical and experimental backgrounds of two-photon absorption (TPA) and TPA-induced free carriers in silicon are presented in detail. In particular, the mostly recent experimental achievements in applications of TPA and TPA-induced free carriers are discussed, such as optical limiting, optical pulse shaping, all-optical switching and modulation, all-optical logic gates, all-optical wavelength conversion and some applications of TPA in silicon photodiode. We show that TPA and TPA-induced free carriers in silicon can provide novel functional devices on chip scale, which would play important roles in the future optical communication and optical signal process systems.

1. Introduction

Intrinsic high optical nonlinearity fortified by tight mode confinement and prospect of dense on-chip integration with microelectronics have made silicon photonics a rapidly growing field [1]. Due to the high-index contrast between the silicon core and silica cladding, silicon waveguides allow strong optical confinement and large effective nonlinearity, which facilitates low cost chip-scale demonstration of all-optical nonlinear functional devices at relatively low pump powers. All-optical signal processing based on nonlinear effects is important to overcome the physical speed limitations of the electronics. If silicon on insulator based waveguides are properly designed, the nonlinear parameter can be up to 7×10^6 W^{-1}·km^{-1} [2], which is more than three orders of magnitude larger than for state-of-the-art highly nonlinear fibers. In the past few years it has been increased and renewed in nonlinear silicon photonics, mainly motivated by the recent technological and experimental advancements in development of next generation high-speed all-optical devices. In fact, nonlinear photonic phenomena and devices in silicon, such as Raman amplification and lasing [3-6], optical modulation [7-8], parametric wavelength conversion and amplification [9-11], all-optical switching [12-14], pulse compression [15-16] and control of slow light [17-18] and so on, have been successfully demonstrated.

At telecommunication wavelength, two-photon absorption (TPA) in silicon is an instantaneous nonlinear loss mechanism dominating at high optical intensities, which are often required to induce Kerr and Raman nonlinearities in aforementioned nonlinear optical devices.

Free carrier absorption (FCA) induced by TPA will also introduce additional loss, so it has often been considered as a fundamental limitation for nonlinear silicon photonic devices [6,9,11,19,20] in optical communication and information processing systems. However, engineered utilization of TPA and FCA induced by TPA may provide new capabilities of silicon photonics in different applications, which have been demonstrated recently. Here we provide the main theoretical and experimental advancements in applications of TPA in silicon photonic devices.

2. Theory of TPA and TPA-induced Free Carriers

2.1 The Principle of TPA
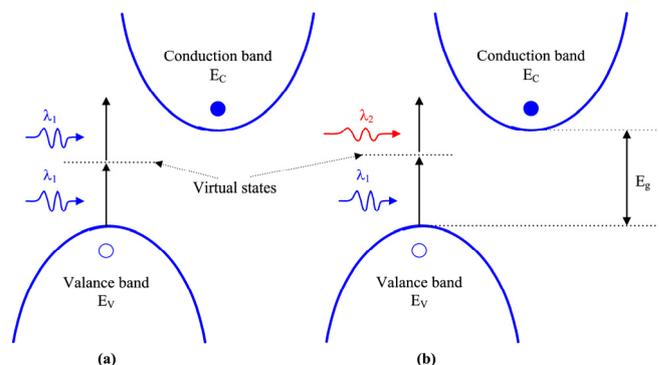
Fig.1. Schematic illustration of TPA in silicon. (a) degenerate TPA.(b) non-degenerate TPA.

Because of its crystal inversion symmetry, the lowest-order nonlinearity in crystalline silicon originates from

third susceptibility. In the presence of a single and two input signals, the third-order nonlinear polarization P related TPA in the silicon waveguide is given [21]

$$P^{(3)}(\omega) = \varepsilon_0 \frac{3}{4} \chi^{(3)}(-\omega; \omega, -\omega, \omega)|E_\omega|^2 E_\omega \quad (1)$$

$$P^{(3)}(\omega_2) = \varepsilon_0 \frac{3}{2} \chi^{(3)}(-\omega_2; \omega_1, -\omega_1, \omega_2)|E_{\omega_1}|^2 E_{\omega_2} \quad (2)$$

where ε_0 is the permittivity of free space and $\chi^{(3)}$ is third order susceptibility tensor. The former equation describes Kerr effect and degenerate TPA, and the later corresponds to non-degenerate Kerr and TPA effects. TPA and Kerr effects are related to the imaginary part and the real part of $\chi^{(3)}$ that correspond to the optical intensity dependence of the optical absorption and the refractive index, respectively. Fig. 1 shows the schematic TPA process in silicon. When the total energy of input two photons is greater than the bandgap energy of silicon ($E_g = E_c - E_v \approx 1.12$ eV), they will be absorbed and excite an electron from the valence band to the conduction band, resulting in generation of a free carrier (electron-hole pair). Depending on the parity difference in the initial and final sates, three types of two-photon transitions can occur, which are referred to as allowed-allowed (a-a), allowed-forbidden (a-f) and forbidden-forbidden (f-f). The TPA coefficient $\beta(\omega) = [3\pi/(c\varepsilon_0\lambda n_0^2)]\text{Im}\{\chi^{(3)}\}$ is a fundamental parameter to evaluate TPA. Considering three types two-photon processes, the total TPA coefficient is given by $\beta(\omega) = \sum_{n=0}^{2} \beta^{(n)}(\omega)$, with n=0, 1 and 2 for a-a, a-f and f-f transitions [22-24], respectively. Because $\beta^{(n)}(\omega) = 2CF_2^{(n)}(h\omega/E_g)$ incorporates a material-dependent constant C, the contribution of each type process is determined by the fundamental photon energy $h\omega$. In the expression of the above equation, $F_2^{(n)}(x) = [\pi(2n+1)!!/2^{n+2}(n+2)!](2x)^{-5}(2x-1)^{n+2}$, $x = h\omega/E_g$, for parabolic electron and hole bands. Assuming that phonon energies are $\ll E_g$, the f-f process is weaker than the two other processes, but it gets its maximum at $h\omega \approx 5E_g/2$[24]. The other two processes become stronger when photon energies are near E_g. In the degenerate TPA, two photons with the same wavelength are absorbed, and the power of the input light will be depleted along the silicon waveguide. A lot of experimental and theoretical works related to degenerate TPA in semiconductors have been carried out. It should be noted that due to the off-diagonal elements in the third-order susceptibility tensor, the TPA exhibits optical polarization dependence, and the presence of TPA anisotropy in silicon was observed [25]. Up to now, z-scan technique and pulse transmission method are used to measure or elevate the TPA coefficient

of silicon. The measured TPA coefficients are summarized in Fig.2.
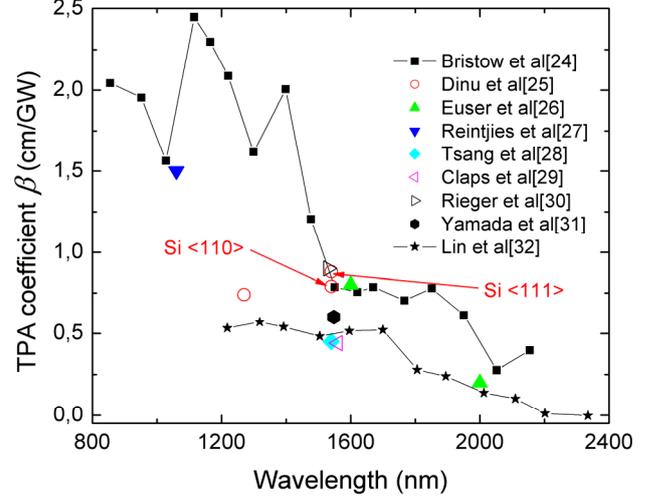
Fig. 2. Measured TPA coefficients at different wavelengths.

In the non-degenerate TPA process, the absorption of a signal is change by a second pump signal instead of by the signal itself, which means that a signal photon is absorbed as a pump photon is present and leads to cross-absorption. From Eq. (2), the non-degenerate TPA process is two times stronger than the degenerate TPA process. It should be pointed out that the non-degenerate TPA is polarization dependent and the linearly polarized beams show stronger polarization dependence than the circularly polarized ones [33-36].

2.2 TPA-induced FCA

TPA process in silicon leads to the generation of free carriers, whose density depends on the incident optical intensity, resulting in FCA loss and free-carrier dispersion (FCD). However, diffusion will reduce the carrier density at the center of the optical mode. The dynamics of free carriers induced by TPA can be described by the Drude model [37-38]. Since the TPA-induced free carriers in the silicon waveguide vary slowly along the z propagation direction, lateral diffusion (along x axis) will dominatedly impact the free-carrier density. The time dependence of equation for the free carrier density in the silicon waveguide is given in terms of free carrier generation and recombination [39]:

$$\frac{dN}{dt} = \frac{\beta I^2}{2h\nu} + D' \frac{\partial^2 N}{\partial x^2} - \frac{N}{\tau_0} \quad (3)$$

where $h\nu$ is the photon energy, I is the optical intensity (time and space dependent), D' is the effective diffusion constant of the free carriers, τ_0 is the carrier recombination

time. Free carriers are accumulative inside the silicon waveguide. For CW signals or pulse signals whose pulse widths are wider than τ_0, free carrier density will be stabilized at a local position with value of $N(z) = \tau_0 \beta I^2(z)/(2h\nu)$ after τ_0 period. For pulse signals whose pulse widths are much narrower than τ_0, we must consider the repetition rate R of the pulse [40, 41]. When the pulse signals operate at low repetition rate ($R\tau_0 \ll 1$), the free carrier density is time dependent and the peak density depends on the pulse width, just like a single pulse, as shown in Fig. 3 (a). When the pulse high repetition rate increases, those free carriers generated by the former pulses may have no enough time to recombine, which will impact the later pulses, as shown in Fig. 3(b).

(a)Evolution of low repetition rate pulses

a

(b)Evolution of high repetition rate pulses

b
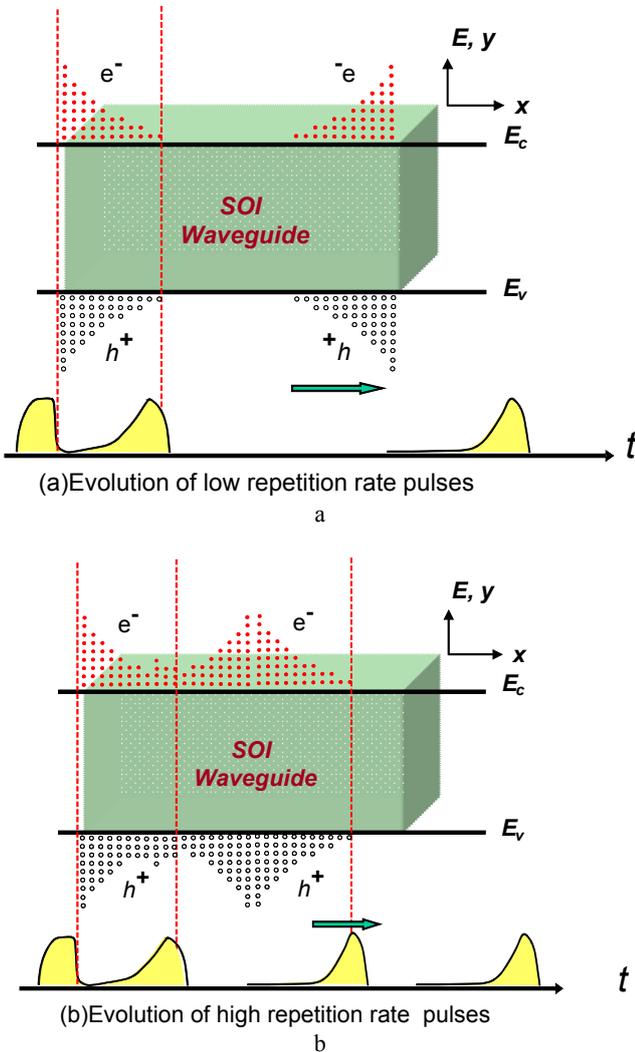
Fig. 3 Evolution of pulses inside the silicon waveguide.

The carrier recombination lifetime τ_0 is a critical parameter influencing the key performance of the nonlinear silicon waveguide photonic devices through limiting the efficiencies of nonlinear effects [6,11,20,29, 40-41]. To overcome free carrier limitation, short pulses are adopted as pump to allow time for recombination between pulses [3, 42-43]. However, the effective carrier recombination time is not a constant in the silicon waveguides, which is in the range from 100 ns to 55 ps [44], depending on different kinds of silicon waveguides. In fact, the effective carrier recombination lifetime is composed of carrier relaxation time, the carrier diffusion time and the surface recombination time [45], so three possible ways can be used to reduce the effective carrier recombination lifetime. Up to now several methods are proposed to reduce free carrier density at high optical intensity by reducing free-carrier recombination time in silicon with ion implantation [44-47], scaling the waveguide for a shorter effective carrier recombination time [48-51], or applying a reverse voltage bias to sweep out the TPA-generated carriers [6, 52-55].

Free carriers induced by TPA are inevitable in silicon at the high optical intensity, which give rise to optical absorption and are responsible for plasma dispersion effect. The absorption loss and the refractive index change induced by free carriers are given by [37]:

$$\alpha_{FC} = \frac{e^3 \lambda^2}{4\pi^2 c^2 \varepsilon_0 n} \left(\frac{\Delta N_e}{m_{ce}^2 \mu_e} + \frac{\Delta N_h}{m_{ch}^2 \mu_h} \right) \tag{4}$$

$$\approx 1.45 \times 10^{-17} \left(\frac{\lambda}{1550} \right)^2 N(z,t)$$

$$\Delta n_{FC} = -\frac{e^2 \lambda^2}{8\pi^2 c^2 \varepsilon_0 n} \left(\frac{\Delta N_e}{m_{ce}} + \frac{\Delta N_h}{m_{ch}} \right) \tag{5}$$

$$\approx -8.2 \times 10^{-22} \lambda^2 N(z,t)$$

So the dispersion induced by free carriers is given by

$$\Delta D_{FC} = \frac{1}{c} \frac{\partial \Delta n_{FC}}{\partial \lambda} = -5.46 \times 10^{-30} \lambda N \tag{6}$$

Because the TPA in silicon is intensity-dependent, both FCA loss and FCD depend on the optical intensity. During propagation inside the waveguide, the optical intensity $I(z,t)$ decreases due to linear absorption and scattering, TPA and FCA. The evolution of the optical signal intensity along the waveguide may be described as

$$\frac{dI(z,t)}{dz} = -\alpha I(z,t) - \alpha_{FC} I(z,t) - \beta I^2(z,t) \tag{7}$$

where α is the linear loss coefficient. Based on the above analysis, when 5 ps optical pulses at 1550 nm input a 1 cm silicon waveguide with free carrier lifetime of 300 ps and effective mode area of 0.10 μm^2, the evolution of FCD and FCA loss along the waveguide at two groups pulse values are shown in Fig. 4 [40].
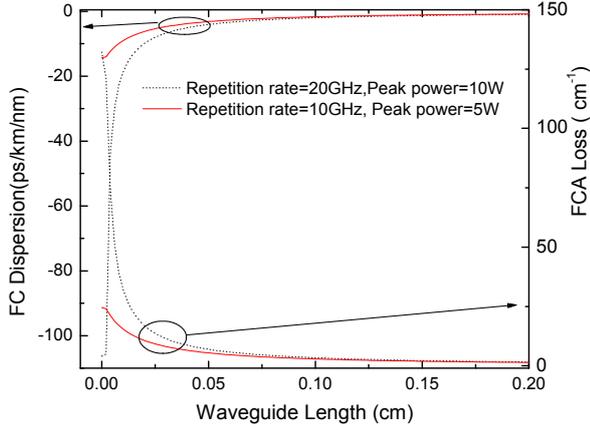
Fig.4 FCD and FCA loss evolution along the waveguide [40].

Fig. 5. Measured output power as a function of the input power.

3. Applications

3.1 Optical limiting

TPA is one of the effective approaches for optical limiting. Compared with other optical limiting mechanisms, the distinct advantage with TPA is that the transmissivity can be high for relatively weak signals because TPA and TPA-induced FCA are small and the silicon devices can be almost completely transparent. From Eq.(7), we can know that the output optical intensity is a function of the input intensity. Because both TPA and TPA-induced FCA is intensity-dependent, the high input intensity means strong TPA and TPA-induced FCA. This is the principle to realize optical limiting performances in silicon waveguides with the TPA and TPA-induced FCA processes. We should point out that if the input signal is a series of optical pulses with given pulse shape, the transmitted pulse shape can change because the nonlinear interactions such as self-phase modulation and free-carrier dispersion etc. With a 1.7 cm silicon waveguide with the effective area of ~5 μm^2, optical limiting characteristics are analyzed experimentally. When laser pulses of ~550 fs are input the waveguide, the relation between the output power and the launched power is given in Fig.5.

3.2 Optical pulse shaping

When optical pulses are input the silicon waveguide, the transient behaviors of TPA and TPA-induced free carriers will have prominent effect on the final output pulses. From Fig.3(a), we can see that upon entering the silicon waveguide the front edge of the pulse will be slightly attenuated by TPA and hence the free carriers will start to accumulate whether the optical energy is present or not. Since free carrier recombination time is much larger than the optical pulse widths, the generated free carriers accumulate and introduce time dependent attenuation along the pulse. As a result, the trailing edge of the pulse entering silicon waveguide is attenuated by TPA and free carriers are created by the front edge of the same pulse. This transient behavior of free carrier concentration will build up over the pulse duration every time the pulse propagates through the silicon waveguide and facilitate a self-compression and modelocking inside a laser cavity. To further understand the pulse shaping, the pulse envelope evolution in the silicon wavegudie can be analyzed through the following nonlinear Schrödinger equation [12,16]:

$$\frac{\partial E(z,t)}{\partial z} = -\frac{1}{2}\left[\alpha + \alpha_{FC}(z,t) + \alpha_{TPA}(z,t)\right]E(z,t) - i\gamma\left|E(z,t)\right|^2 E(z,t) + i\frac{2\pi}{\lambda}\Delta n_{FC}(z,t)E(z,t) \tag{8}$$

where $\alpha_{TPA}(z,t) = \ln(1+\beta I_0 z)/z$ and γ are attenuation coefficient by TPA and Kerr nonlinear coefficient, respectively. Based on the peak pulse intensity and pulse energy, the nonlinear response in silicon can be divided into TPA dominated regime and FCA dominated regime [16,56]. Fig.6 (a) shows the calculated results of two regimes for 20 ps and 500 ps optical pulses with 1 kW peak power. The waveguide is 1 cm long with 5 μm^2 effective area and 16 ns free carrier recombination time

[16]. 20 ps pulses are broadened due to TPA dominance and 500 ps pulses are compressed to 350 ps by FCA dominance. The FC dispersion causes a linear phase change across the pulse. Fig.6 (b) illustrates the pulse compression for 100 ps optical pulses at different optical intensity with different waveguide length [16]. At low intensity, stronger TPA induced pulse broadening is over FCA induced pulse self-compression. FCA dominance can be achieved at higher intensities and facilitate pulse compression.
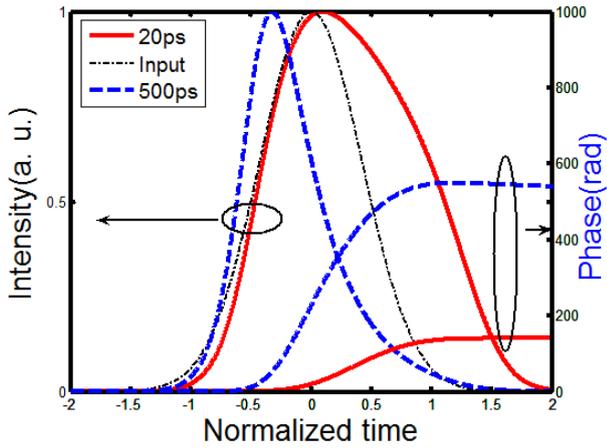
a
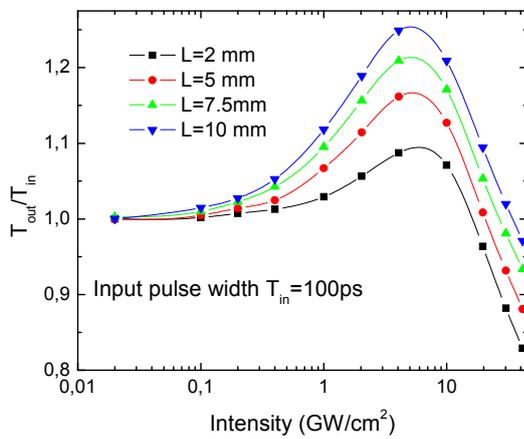
b

Fig. 6. (a) Output pulses and phase induced by TPA and free carriers. (b) Predicted pulse compression in silicon waveguides [16].

oscilloscope (DSO) to measure the output pulse characteristics. Fig.7(b) shows that the 1.5 ns pulse can be compressed to 60 ps [16].
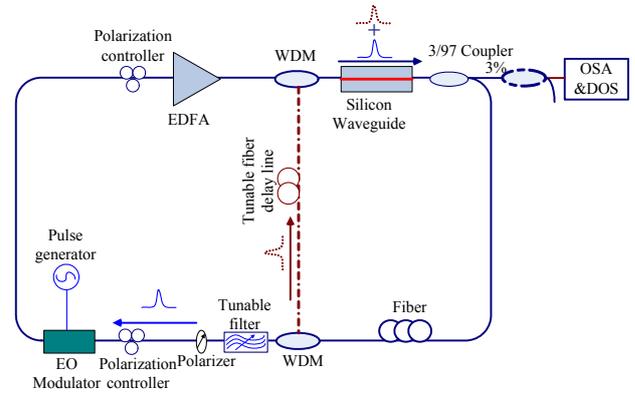
a
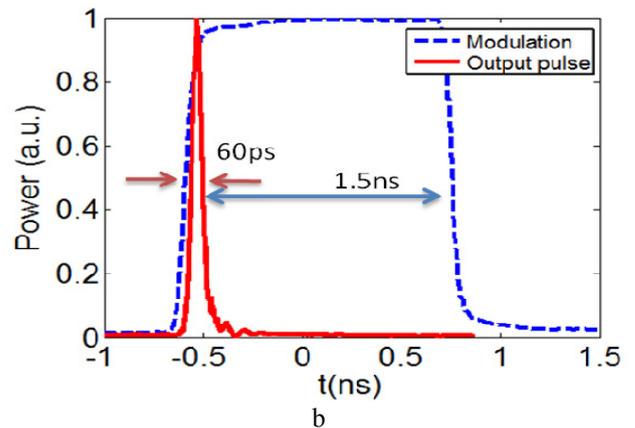
b

Fig.7 (a) Schematic of the experimental setup. (b) Compressed pulse for 1.5 ns input pulse[15].

The schematic of experimental setup is shown in Fig. 7(a). The silicon waveguide has a p-i-n diode structure to inject carriers and hence a modulation capability. The output of the waveguide is connected to a 3/97 tap coupler where 3% used as an output and 97% is fed into the gain medium, a high power erbium doped fiber amplifier (EDFA). A resonator is formed by launching the EDFA output back into the silicon waveguide input end. An optical bandpass filter is inserted to insure lasing at a desired wavelength and suppress undesired ASE accumulation. Since the pulse shaping by free carriers requires time varying optical signal circulating inside the laser cavity, an electro-optic (EO) modulator is connected to the waveguide to start initial pulsation. The output pulse width is expected to be minimum when the frequency of the function generator matches the fundamental cavity frequency. Here, frequency locking is achieved manually by monitoring the pulse shape and the modulation frequency, simultaneously. The output of the resonator is connected to an optical spectrum analyzer (OSA) and a photodetector followed by a 25 GHz digital sampling

Once the short pulses are generated, we are able to utilize them as pump to achieve stimulated Raman scattering and mode locking in the same silicon waveguide. Because of the wavelength selectivity of the filter and other optics inside the EDFA, another cavity for Raman Stokes pulse is needed. The original laser cavity is modified by using two WDM couplers, which separate the Stokes from the wavelength sensitive components in the pulse compression cavity and recombine before the silicon waveguide, and a tunable fiber delay line as shown in Fig. 7(a), to facilitate resonance at the pump wavelength and the Stokes wavelengths. After pulses When both waves are aligned temporally, we observe dual wavelength lasing [57]. The spectra of the dual wavelength laser are shown in Fig. 8 [57]. The pump wavelength is selected by the bandpass filter inside the laser cavity at 1540 nm and the expected Raman Stokes signal is at wavelength of 1675 nm. Since free carriers are created and accumulate in the silicon waveguide, the Raman Stokes pulse also suffers from free carrier attenuation. Therefore, the final outcome of the Raman Stokes pulses is the combination of Raman amplification, TPA, and FCA.
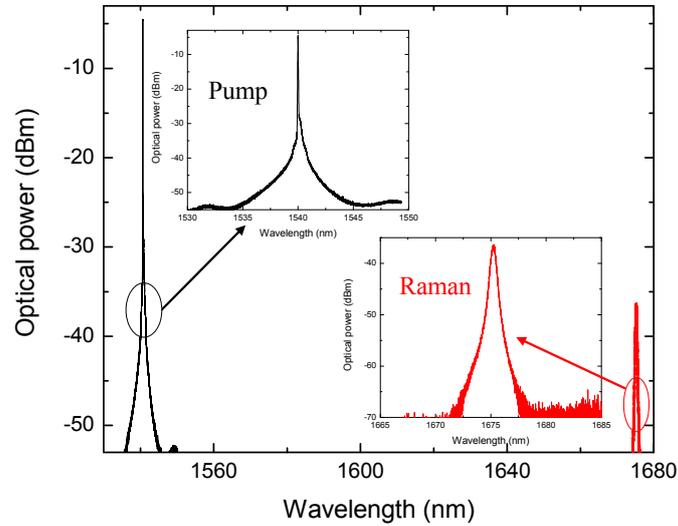
Fig.8. Spectra of pulse-compressed pump and Raman laser [57].

3.3 All-Optical Switching and Modulation

All-optical switching and modulation facilitate ultrafast signal processing by overcoming the limitations of optical-to-electronic conversion, which are important components in the optical communication and signal-processing systems. In recent years, most of the reported silicon based optical switching and modulation are based on free carrier dispersion effect introduced inside the silicon waveguide by either external current injection or optical excitation [7-8,14,58-74]. Modulation of light by light in silicon waveguides was demonstrated with visible light, which was based on free carrier dispersion induced by single photon absorption [68-69]. Similarly, fast all-optical switching in silicon microring resonators was demonstrated with a pump laser at 800 nm [44,65-66]. To achieve the required phase shift or absorption in silicon based all-optical switches and modulators rely on TPA and TPA-induced free carriers, a relative strong pump light is need, and the switching time or the response time is limited by the effective free carrier recombination lifetime generally. To overcome this limitation, some measures should be used to reduce the free carrier recombination lifetime, such as short pulse, reverse voltage bias, ion-implanted waveguide and so on. In addition to the demonstrated all-optical switches and modulators based on free carrier dispersion, these devices using a direct TPA process have also been demonstrated [13, 72-74], which show that the possible response speeds are not limited by the effective carrier recombination lifetime. Table 1 presents a summary of the demonstrated silicon-based all-optical switches and modulators relaying on TPA.

Table 1.   Demonstrated all-optical switches and modulators in silicon waveguide.

Author	Waveguide structure	Modulation depth	Response time	peak pump power	Principle
Tanabe et al [51, 70]	Photonic crystal nanocavities	~90%	~50 ps	<150 mw	TPA induced FC dispersion
Hache et al [71]	Photonic crystal	-	~12ps	~500KW	TPA induced FC dispersion
Tanabe et al [45]	Ion-implanted photonic crystal nanocavities	~78%	~70 ps	~60 mW	TPA induced FC dispersion
Liang et al[13]	Strip nanowire waveguide	70%	<3 ps	1.9 W	TPA
Nunes et al [72,73]	Strip nanowire waveguide	92%	1.9 ps	~1.5W	TPA
Almeida et al [8]	M-Z interferometer	~68%	~20 ps	~133 W	TPA induced FC dispersion
Preble et al [54]	Microring resonators	~84%	~122ps	800 mW	TPA induced FC dispersion
Moss et al [74]	Rip waveguide	>80%	<15 ps	1.2 kW	TPA

3.4 All-Optical Logic Gates

(a)

(b)

NOR		
P1	P2	Out
0	0	1
0	1	0
1	0	0
1	1	0

(c)
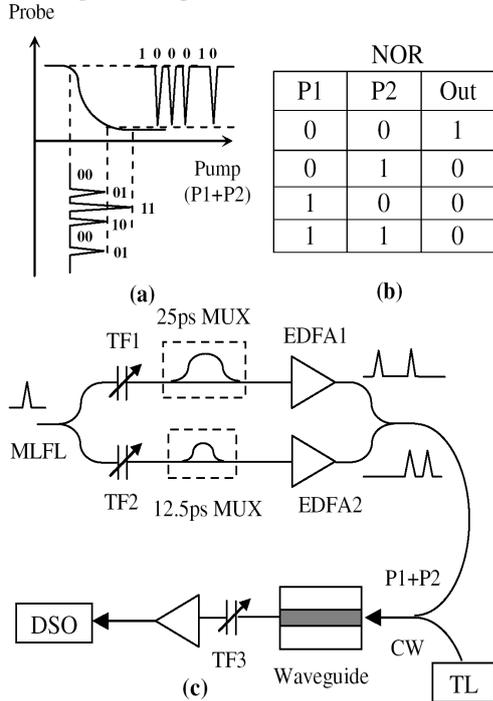
Fig. 9. (a) Operating principle. (b) Truth table. (c) Experimental setup.

All-optical logic gates are important devices for performing all-optically arithmetic operations in the future optical signal processing process systems to overcome the speed limitations of electronics. Up to now, all-optical logic gates based on TPA and TPA-induced free carrier dispersion effect are reported [21,75-77]. For the all-optical logic NOR gate based on the nonlinear transmission characteristics of TPA in silicon, The operating principle and experimental schematic diagram are depicted in Fig.9 [75]. Signals P1 and P2 with the same peak power are combined together and coupled into the silicon waveguide. The weak CW probe light is modulated by P1 and P2 by means of non-generate TPA effect. As long as one of two pump signals is bit "1" (includes"01", "10" and "11"), optical absorption on the probe light will be introduced. Once P1and P2 are both bit "0", the probe light will transmit though the silicon waveguide without additional nonlinear loss. Fig.10 shows the experimental results [75]. The direct application of TPA allows high-speed operation, which is not limited by the free carrier lifetime in the silicon waveguide.
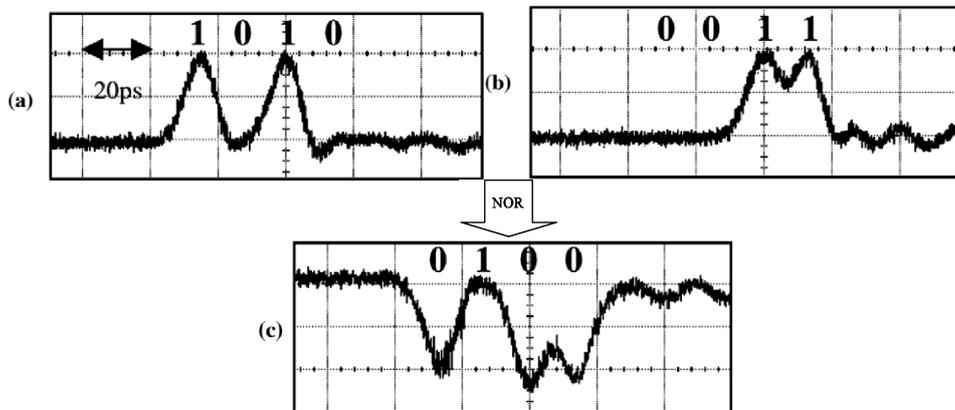
Fig. 10. (a) Signal P1. (b) Signal P2. (c) Output CW probe with logic NOR operation [75].
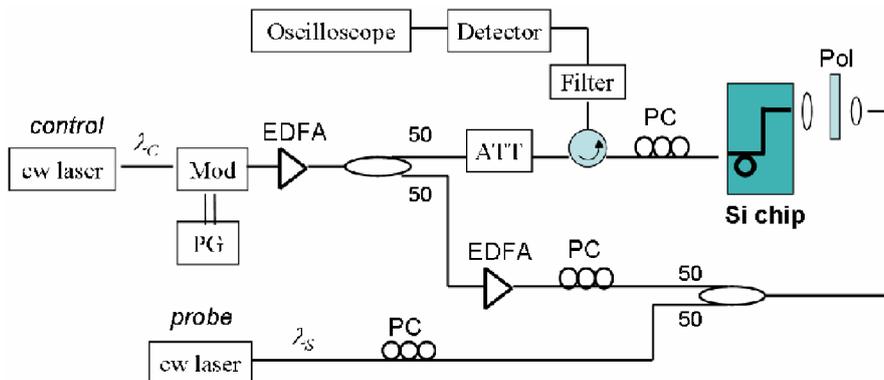
Fig. 11. Experimental setup for all-optical logic AND and NAND operations in silicon ring resonator.

Silicon micro-resonating structures can enhance power density, slow down the pulse propagation and reduce the effective free carrier lifetime, so that the nonlinear response is larger and more compact devices can be realized. Recently, all-optical logic AND and NAND Gates at 310 Mb/s have been demonstrated based on TPA-induced free carrier dispersion effect in silicon micro-ring resonates [77]. As a control pulse and a weak CW probe light are combined into the ring resonator though two different resonances, the generated free carriers due to TPA decrease the refractive index of the silicon. After the control pulse leaves the resonant wavelength and the transmission of the probe light relax back due to the

recombination of the free carriers. The experimental setup is shown in Fig.11 [77]. As both control signals are bit "1", the total power is larger than threshold to achieve large modulation, a positive or negative modulation is imposed on the probe light. When one or both of the control signals are bit "0", the total optical power is less than the threshold, and small modulation is observed on the probe output. This results in the AND and NAND operations at different resonance wavelengths, as shown in Fig.12. It should be noted that the bit-rate is limited by the effective free carrier recombination lifetime, and some measures can be used to reduce the effective carrier lifetime and to obtain higher bit rate.
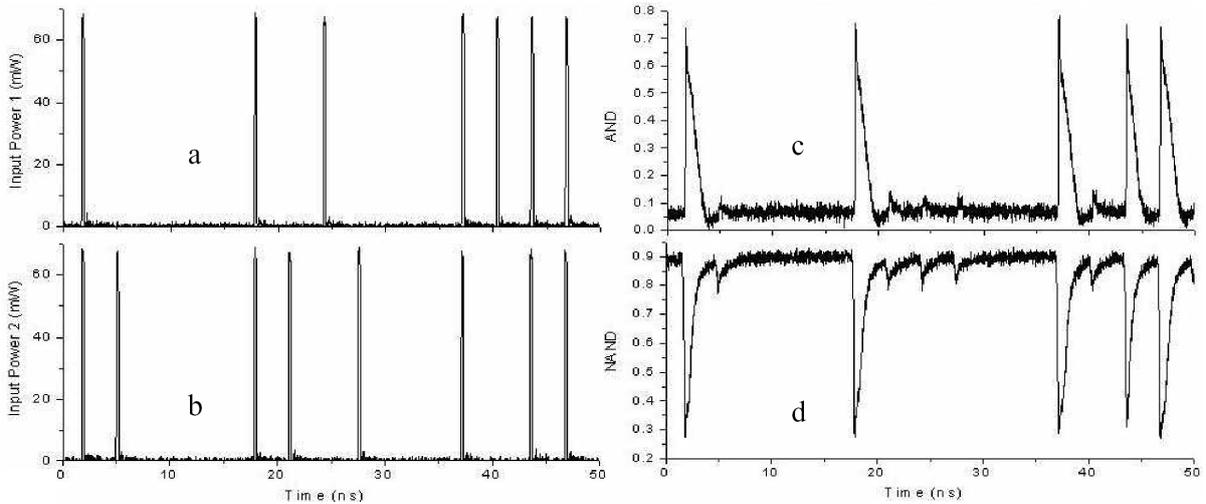
Fig.12. (a) Control signal 1. (b) Control signal 2. (c) Probe light output at $\lambda_{Probe} = \lambda_{P1}$ as the logic AND operation. (d) Probe light output at $\lambda_{Probe} = \lambda_{P2}$ as the logic NAND operation [77].

3.5 All-Optical Wavelength Conversion
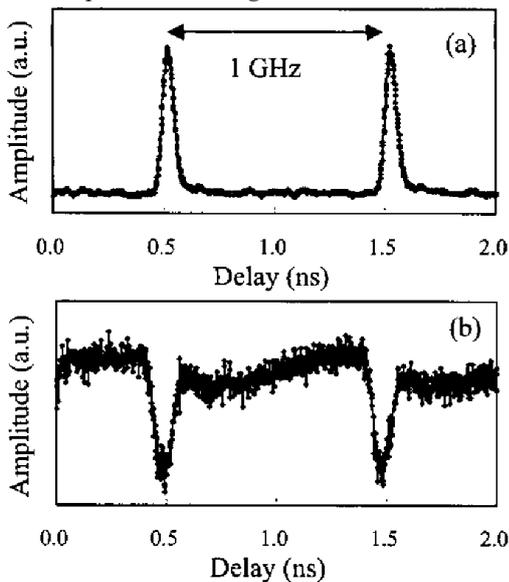
Fig.13 (a) Pump signal at 1550 nm. (b) Converted signal at 1544 nm[81].

All-optical wavelength conversion is considered to be an essential functionality for the future all-optical switching architectures. Many all-optical wavelength conversion schemes based on nonlinear effects in the highly nonlinear fibers were demonstrated [78]. All-optical conversions in silicon wavegudies are based on four-wave mixing have been investigated in the last several years [9-11,55,56, 79,80]. In the wavelength conversion based on cross absorption modulation via the non-degenerated TPA process, the modulated pump signals can be copied to the probe light inversely [81,82]. When the 1 GHz pump light at 1550 nm and the probe light at 1544 nm are collinearly coupled into a 1.0-cm long silicon waveguide, the converted signal is given in Fig.13 [81]. Recently, 10 Gb/s pump light at 1552.52 is converted to the probe light at 1320 nm [82]. Based on the free carrier dispersion effect induced by TPA, highly integrated micrometer-scale low power wavelength conversion at 0.9 Gb/s in a silicon ring resonator with average power of 4.5 mW was also demonstrated [83].

3.6 Applications of TPA in a Silicon Photodiode

TPA in silicon photodiode has been widely investigated as an inexpensive, ultrafast, ultrasensitive and flexible technique, which is exploited for applications such

as pulse shape measurement [84-85], optical clock recovery [86-88] and dispersion measurement [89-92]. Since TPA is a fast nonresonant effect and does not require phase matching between input singals, it can provides broadband operations. Even without the use of lock-in detection, 1.5×10^{-3} (mW)^2 peak-power times average power sensitivity in nonlinear autocorrelation measurements via direct TPA in a single photon counting silicon photodiode can be realized [85]. Automatic dispersion control for 160 Gb/s transmission can be achieved based on dispersion measurement with TPA in the silicon photodiode [90-92]. Optical clock recovery is a prerequisite for optical demultiplexing, optical logic and optical retiming etc. The principle of clock recovery via TPA is depicted in Fig.14 [87]. The cross-correlation between data stream and an optical clock signal, measured using TPA in the silicon avalanche photodiode. The correlated signal exhibits a background level caused by TPA of the clock and data separately. To achieve clock recovery, the offset was subtracted to produce a bipolar cross-correlation signal, which is used as the error signal in a phase-locked loop to synchronize the clock and data. With this method, a 10 GHz optical clock is synchronized to an 80 Gb/s data stream over 840 km transmission fiber [88].
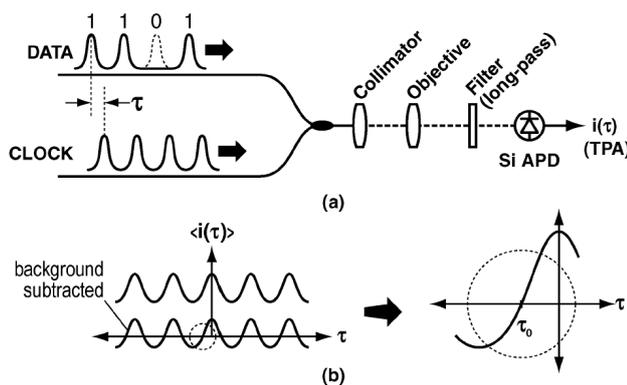
Fig. 14. Schematic diagram to measure timing difference between data and clock signals[87].

4. Conclusion

Although TPA and TPA induced free carriers are often considered to be a fundamental limitation degrading the performance of the nonlinear photonic devices based on optical Kerr and Raman effects, they can also provide a novel way to realize novel functional devices. Theoretical background of TPA and TPA-induced free carriers is presented in detail. It has been shown that many functional devices based on TPA and TPA-induced free carriers have been successfully demonstrated, and some of them show noticeable advantages over those with traditional methods. With further development of the silicon waveguide techniques, these devices based on TPA and TPA-induced free carriers will play important roles in the future high speed optical communication network and optical signal processing systems.

References

[1] G. T. Reed, Nature **427**, 595 (2004).
[2] C. Koos, L. Jacome, C. Poulton, J. Leuthold, W. Freude, Opt. Express **15**, 5976 (2005).
[3] O. Boyraz, B. Jalali, Electron. Express **1**, 429 (2004).
[4] A. Liu, H. Rong, R. Jones, O. Cohen, D. Hak, M. Paniccia, J. Lightwave Technol. **24**, 1440 (2006).
[5] O. Boyraz, B. Jalali, Opt. Express **12**, 5269 (2004).
[6] H. Rong, R. Jones, A. Liu, O. Cohen, D. Hak, A. Fang, M. Paniccia, Nature **433**, 725 (2005).
[7] R. Jones, A. Liu, H. Rong, M. Paniccia, Opt. Express **13**, 1716 (2005).
[8] V. R. Almeida, Q. Xu, M. Lipson, Opt. Lett. **30**, 2403 (2005).
[9] M. A. Foster, A. C. Turner, J. E. Sharping, B. S. Schmidt, M. Lipson, A. L. Gaeta, Nature **441**, 960 (2006).
[10] K. Yamada, H. Fukuda, T. Tsuchizawa, T. Watanabe, T. Shoji, S. Itabashi, IEEE Photon. Technol. Lett. **18**, 1040 (2006).
[11] K. K. Tsia, S. Fathpour, B. Jalali, Opt. Express **14**, 12327 (2006).
[12] O. Boyraz, P. Koonath, V. Raghunathan, B. Jalali, Opt. Express **12**, 4094 (2004).
[13] T. K. Liang, L. R. Nunes, T. Sakamoto, K. Gasagawa, T. Kawanishi, M. Tsuchiya, Opt. Express **13**, 7298 (2005).
[14] R. Dekker, A. Driessen, T. Wahlbrink, C. Moormann, J. Niehusmann, M. Forst, Opt. Express **14**, 8336 (2006).
[15] E. Tien, N. S. Yuksek, F. Qian, O. Boyraz, Opt. Express **15**, 6500 (2007).
[16] E. Tien, F. Qian, N. S. Yuksek, O. Boyraz, Appl. Phys. Lett. **91**, 201115-1-3 (2007).
[17] Y. Okawachi, M. A. Foster, J. E. Sharping, A. L. Gaeta, Opt. Express **14**, 2317 (2006).
[18] F. Xia, L. Sekaric, Y. Vlasov, Nature Photonics **1**, 65 (2007).
[19] T. K. Liang, H. K. Tsang, Appl. Phys. Lett **84**, 2745 (2004).
[20] S. Fathpour, K. K. Tsia, B Jalali, IEEE J. Quantum Electron. **43**, 1211 (2007).
[21] P. Dumon, G. Priem, L. R. Numers, W. Bogaerts, D. V. Thourhout, P. Bienstman, T. K. Liang, M. Tsuchiya, P. Jaenen, S. Beckx, J. Wouters, R. Beats, Jpn. J. Appl. Phys.**45**, 6589 (2006).
[22] M. Sheik-Bahae, D. J. Hagan, E. W. Van Stryland, Phys. Rev. Lett. **65**, 96 (1990).
[23] H. Carcia, R. Kalyanaraman, J. Phys. B: At. Mol. Opt. Phys. **39,** 2737 (2006).
[24] A. D. Bristow, N. Rotenberg, H. M. van Driel, Appl. Phys. Lett. **90**, 191104-1-3 (2007).
[25] M. Dinu, F. Quochi, H. Garcia, Appl. Phys. Lett. **82**, 2954 (2003).
[26] T. G. Euser, W. L. Vos, J. Appl. Phys. **97**, 043102-1-7 (2005).
[27] J. F. Reintjes, J. C. McGroddy, Phys. Rev. Lett. **30**, 901 (1973).

[28] H. K. Tsang, C. S. Wong, T. K. Liang, I. E. Day, S. W. Roberts, A. Harpin, J. Drake, M. Asghari, Appl. Phys. Lett. **80**, 416 (2002).

[29] R. Claps. D. Dimitropoulos, V. Raghunathan, Y. Han, B. Jalali, Opt. Express **11**, 1731 (2003).

[30] G. W. Rieger, K. S. Virk, J. F. Young, Appl. Phys. Lett. **84**, 900-902(2004).

[31] H. Yamada, M. Shirane, T. Chu, H. Yokoyama, S. Ishida, Y. Arakawa, Jpn. J. Appl. Phys. **44**, 6541 (2005).

[32] Q. Lin, J. Zhang, G. Piredda, R.W. Boyd, P. M. Fauchet, G. P. Agrawal, Appl. Phys. Lett. **91**, 021111-1-3 (2007).

[33] M. Sheik-Bahae, J. Wang, E. W. Van Stryland, IEEE J. Quantum Electron. **30**, 249 (1994).

[34] E. Tien, O. Boyraz, Proceeding of Group IV Photonics Conference(Optical society of America, 2006) pp.58-60, 2006.

[35] R. Salem, T. E. Murphy, Opt. Lett. **29**, 1524 (2004).

[36] T. Kagawa, S. Ooami, Jpn. J. Appl. Phys. **46**, 664 (2007).

[37] R. A. Soref, B. R. Bennett, IEEE J. Quantum Electron.**23**, 123 (1987).

[38] A. J. Sabbah, D. M. Riffe, Phys. Rev. B **66**, 165217-1-11 (2002).

[39] Y. Liu, H. K. Tsang, Appl. Phys. Lett **90**, 211105-1-3 (2007).

[40] X. Sang, O. Boyraz, Opt. Express **16**, 13122 (2008).

[41] L. Yin, G. P. Agrawal, Opt. Lett. **32**, 2031-2033(2007).

[42] Q. Xu, V. R. Almeida, M. Lipson, Opt. Lett. **30**, 35 (2005).

[43] T. K. Liang, H. K. Tsang, Appl. Phys. Lett. **85**, 3343 (2004).

[44] M. Fost, J. Niehusmann, T. Plotzing, J. bolten, T. Wahlbrink, C. Moormann, H. Kurz, Opt. Lett. **32**, 2046 (2007).

[45] T. Tanabe, K. Nishiguchi, A. Shinya, E. Kuramochi, H. Inokawa, M. Notomi, Appl. Phys. Lett. **90**, 031115-1-3 (2007).

[46] D. H. Macdonald, H. Maeckel, S. Doshi, W. Brendle, A. Cuevas, J.S. Williams, M. J. Conway, Appl. Phys. Lett. **82**, 2987 (2003).

[47] Y. Liu, H. K. Tsang, Opt. Lett. **31**, 1714 (2006).

[48] R. L. Espinola, J. I. Dadap, R. M. Osgood, Jr., Opt. Express **12**, 3713 (2004).

[49] R. Claps, V. Raghunathan, D. Dimitropoulos, B. Jalali, Opt. Express **12**, 2774 (2004).

[50] D. Dimitropoulos, R. Jhaveri, R. Claps, J. C. S. Woo, B. Jalali, Appl. Phys. Lett. **86**, 071115-1-3 (2005).

[51] T. Tanabe, M. Notomi, S. Mitsugi, A. Shinya, E. Kuramochi, Opt. Lett. **30**, 2575 (2005).

[52] H. Rong, A. Liu, R. Jones, O. Cohen, D. Hak, R. Nicolaescu, A. Fang, M. Paniccia, Nature **433**, 292 (2005).

[53] D. Dimitropoulos, S. Fathpour, B. Jalali, Appl. Phys. Lett. **86**, 261108-1-3 (2005).

[54] S. F. Preble, Q. Xu, B. S. Schmidt, M. Lipson, Opt. Lett. **30**, 2891 (2005).

[55] H. Rong, Y. Kuo, A. Liu, M. Paniccia, Opt. Express **14,** 1182 (2006).

[56] R. Dekker, A. Driessen, T. Wahlbrink, C. Moormann, J. Niehusmann, M. Forst, Opt. Express **14**, 8336 (2006).

[57] X. Sang, E. Tien, F. F. Qian, N. S. Yukseck, Q. Song, O. Boyraz, IEEE Photon. Technol. Lett. **20**, 1184 (2008).

[58] A. Liu, L. Liao, D. Rubin, H. Nguyen, B. Ciftcioglu, Y. Chetrit, N. Izhaky, M. Paniccia, Opt. Express **15**, 660 (2007).

[59] C. Manolatou, M. Lipson, J. Lightwave Technol. **24**, 1433 (2006).

[60] A. Liu, Jones, L. Liu, L. Liao, D. Samara-Rubio, D. Rubin, O. Cohen, R. Nicolaescu, M. Paniccia, Nature **427**, 615 (2004).

[61] A. Irace, G. Breglio, M. Iodice, A. Cutolo, J. Appl. Phys. **94**, 361 (2004).

[62] A. Liu, L. L. Lian, D. Rubin, H. Nguyen, B. Ciftcioglu, Y. Chetrit, N. Izhaky, M. Paniccia, Opt. Express **15**, 660 (2007).

[63] Q. Xu, B. Schmidt, S. Pradhan, M. Lipson, Nature **435**, 325 (2005).

[64] F. C. Ndi, J. Toulouse, T. Hodson, D. W. Prather, Opt. Lett. **30**, 2254 (2005).

[65] A. R. Almeida, C. A. Barrios, R. R. Panepucci, M. Lipson, Nature **431**, 1081 (2004).

[66] A. R. Almeida, C. A. Barrios, R. R. Panepucci, M. Lipson et al, Opt. Lett. **29**, 2867 (2005).

[67] P. Dong, S. F. Preble, M. Lipson, Opt. Express **15**, 9600 (2007).

[68] S. Stepanov, S. Ruschin, Appl. Phys. Lett. **83**, 5151 (2003).

[69] R. Normandin, D. C. Houghton, M. Simard-Normandin, Can. J.Phys. **67**, 412 (1989).

[70] T. Tanabe, M. Notomi, S. Mitsugi, A. Shinya, E. Kuramochi, Appl. Phys. Lett. **87**, 151112-1-3 (2005).

[71] A. Hache, M. Bourgeois, Appl. Phys. Lett. **77**, 4089 (2000).

[72] L. R. Nunes, T. K. Liang, K. S. Abedin, D. Van Thourhout, P. Dumon, R. Baets, H.K. Tsang, T. Miyazaki, M. Tsuchiya, Proc. ECOC 2005, Glasgow, September 2005, PD Th.4.2.3.

[73] T. K. Liang, K. Akahane, N. Yamamoto, L. R. Nunes, T. Kawanishi, M. Tsuchiya, IEICE Trans. Electron. **E90-C**, 409 (2007).

[74] D. J. Moss, L. Fu, I. Littler, B. J. Eggleton, Electron. Lett.**41**, 320 (2005).

[75] T. K. Liang, L. R. Nues, M. Tsuchiya, K. S. Abedin, T. Miyazaki, D. Van Thourhout, W. Bogaerts, P. Dumon, R. Baets, H.K. Tsang, Opt. Comm. **265**, 171 (2006).

[76] T. K. Liang, L. R. Nunes, M. Tsuchiya, K.S. Abedin, T. Miyazaki, D. Van Thourhout, P. Dumon, R. Baets, H. K. Tsang, OFC 2006, Anaheim, CA, March 2006, OFP1.

[77] Q. Xu, M. Lipson, Opt. Express **15**, 924 (2007).

[78] X. Sang, P. Chu, C. Yu, Opt. Quantun Electron. **37**, 965 (2005).

[79] M.A. Foster, A.C. Turner, R. Salem, M. Lipson, A.L. Gaeta, Broad-band continuous-wave parametric wavelength conversion in silicon nanowaveguides, Opt. Express **15**, 12949 (2007).

[80] Y. Kuo, H. Rong, V. Sih, S. Xu, M. Paniccia, Opt. Express **14**, 11721 (2006).

[81] T. K. Liang, L. R. Nunes, H. K. Tsang, M. Tsuchiya, D. Van Thourhout, P. Dumon, R. Baets, W. Gogaerts, Proc. ECOC 2005, Glasgow, September 2005, Paper We4. P.043.

[82] K. Yamada, H. Fukuda, T. Watanabe, T. Tsuchizawa, H. Shinojima, T. Tanabe, M. Takahashi, S. Itabashi, Proceeding of Group IV Photonics Conference 2006, p237-239, 2006

[83] Q. Xu, V. R. Almeida, M. Lipson, Opt. Lett. **30**, 2733 (2005).

[84] K. Kikuchi, Electron. Lett. **34**, 123 (1998).

[85] C. Xu, J. M. Roth, W. H. Knox, K. Bergman, Electron. Lett. **38**, 86 (2002).

[86] R. Salem, G. E. Tudury, T.U. Horton, G.M. Carter, T.E. Murphy, IEEE Photon. Technol. Lett., **17**, 1968 (2005).

[87] R. Salem, T. E. Murphy, IEEE Photon. Technol. Lett. **16**, 2141 (2004).

[88] R. Salem, A. A. Ahmadi, G. E. Tudury, J. Lightwave Technol. **24**, 3353 (2006).

[89] T. Inui, K. R. Tamura, K. Mori, T. Morioka, Electron. Lett. **38**, 1459 (2002).

[90] T. Inui, K. Mori, T. Ohara, H. Takara, T. Komukai, T. Morioka, Electron. Lett. **40**, 256 (2004).

[91] S. Wielandy, M. Fishteyn, T. Her, D. Kudelko, C. Zhang, Electron. Lett. **38**, 1198 (2002).

[92] S. Wielandy, P. S. Westbrook, M. Fishteyn, P. Reyes, W. Schairer, H. Rohde, G. Lehmann, Electron. Lett. **40**, 690 (2004).

[*]Corresponding author: xzsang@gmail.com